Kinetics of Crystal Nucleation and Growth in Thin Films of Amorphous Te Alloys measured by Atomic Force Microscopy

J. Kalb[1,2], F. Spaepen[1] and M. Wuttig[2, a)]
[1]Division of Engineering and Applied Sciences, Harvard University,
Cambridge, MA 02138, U.S.A.
[2]I. Physikalisches Institut der RWTH Aachen, 52056 Aachen, Germany

ABSTRACT

Both the crystal nucleation rate and the crystal growth velocity of sputtered amorphous $Ag_{0.055}In_{0.065}Sb_{0.59}Te_{0.29}$ and $Ge_4Sb_1Te_5$ thin films used for optical data storage were determined as a function of temperature. Crystals were directly observed using ex-situ atomic force microscopy, and their change in size after each anneal was measured. Between 140°C and 185°C, these materials exhibited similar crystal growth characteristics, but differed in their crystal nucleation characteristics. These observations provide an explanation for the different re-crystallization mechanisms observed upon laser-induced crystallization of amorphous marks.

INTRODUCTION

In order to increase the data transfer rate of optical data storage media, the time-limiting factor, which is the re-crystallization of an amorphous bit, has to be accelerated. Therefore, it is essential to understand the mechanisms of re-crystallization of phase change materials. Two mechanisms of re-crystallization depending on the composition of the alloy have been observed. For instance, AgIn-doped Sb_2Te re-crystallizes by the growth of the crystalline phase from the rim of the amorphous bit towards its center [1]. In contrast, $Ge_4Sb_1Te_5$ (an alloy close to the GeTe-Sb_2Te_3 pseudobinary line [2]) re-crystallizes by nucleation and subsequent growth of crystals inside the amorphous bit [3]. The atomistic basis for this difference is still not clearly understood. Even though several research groups have assumed that these alloys differ in their crystal nucleation rate and crystal growth velocity, systematic measurements of these two quantities as a function of temperature have to the best of our knowledge so far not been performed. Therefore, in many modeling studies of re-crystallization the fitting parameters have no direct experimental justification [4-6]. Additional difficulties occur because the glass transition temperature T_g is usually accompanied by an *abrupt* change in the temperature derivative of several physical parameters [7-9]. Therefore, crystallization parameters (in particular activation energies) determined experimentally from the easily accessible amorphous phase (below T_g) cannot be extrapolated into the undercooled liquid (above T_g). Only experimental data collected above T_g are useful for the simulation and understanding of the re-crystallization process of phase change media, which also occurs above T_g. Therefore, there is a strong demand of systematic measurements of the crystallization parameters in the regime of the undercooled liquid (rather than the amorphous phase).

[a)] electronic mails: kalb@deas.harvard.edu, spaepen@deas.harvard.edu, wuttig@physik.rwth-aachen.de

EXPERIMENTAL PROCEDURE

Phase change films with two compositions, namely $Ag_{0.055}In_{0.065}Sb_{0.59}Te_{0.29}$ (hereafter AgInSbTe) and $Ge_4Sb_1Te_5$, and thickness of 30 nm were deposited on 640 µm thick Si (100) substrates by direct current magnetron sputtering. The background pressure was approximately 10^{-6} mbar and the working pressure during sputtering in Ar ambient $7 \cdot 10^{-3}$ mbar. The sputtering power was 100 W. The deposition rate was approximately 0.5 nm/s. The diameter of the sputter target was 10 cm and the target-substrate distance 5 cm. As determined from X-ray diffraction (XRD) measurements, the structure of the as-deposited films was entirely amorphous, i.e. no evidence of partial crystallization during deposition could be observed. The composition of the films was determined by inductive coupled plasma emission spectroscopy and energy dispersive X-ray analysis. The samples were prepared without additional capping layers (in practice, phase change films are sandwiched between thin layers of $ZnS\text{-}SiO_2$).

The samples were partially crystallized by isothermal annealing. Due to the density change upon crystallization, which induces a change in film thickness on the order of 5% [10-11], crystals could be observed as a depression in the amorphous matrix in a Digital Instruments DI 3100 atomic force microscope (AFM) in TappingMode™. Subsequently, the sample was annealed (ex-situ) a second time at the same temperature and rescanned in the AFM at the same microscopic location (this was possible by scratching the film with a fine needle and using the optical microscope attached to the AFM for assistance). The crystal growth velocity was determined as the ratio of the increase in crystal radius and the annealing time. Additional ex-situ annealing/rescanning cycles were performed to establish the time-dependence of the growth velocity. Counting the number of crystals per unit area of the sample surface gave information about the crystal nucleation rate.

Due to the pronounced temperature dependence of the processes studied here, the very precise furnace of a Perkin Elmer Pyris 1 differential scanning calorimeter (DSC) was employed for the anneals between 140°C and 170°C (temperature uncertainty: less than 0.1°C). The sample (4mm x 4mm) was heated up and cooled down at 50 K/min and, depending on the temperature, annealed between several hours and about one minute. High-purity argon was used to provide an inert atmosphere.

For anneals between 170°C and 185°C, which lasted between about one minute and a few seconds, the sample was immersed manually in hot safflower oil and subsequently quenched into room temperature ethylene glycol. The sample (8mm x 4mm) was held by a copper wire (0.5mm diameter), which was coiled two or three times around the sample. The oil was stirred continuously, and its temperature was measured by a mercury thermometer (temperature uncertainty: less than 0.5°C). Oil residues on the sample were cleaned off with an isopropanol-soaked soft cloth after each anneal.

RESULTS AND DISCUSSION

A. AgInSbTe

Figure 1 (a) and 1 (b) show AFM scans taken after anneals at 160°C and 185°C, respectively. At a given time, all crystal diameters are roughly constant. In particular, no smaller crystals are visible in the third picture of each sequence. Therefore, (heterogeneous) nucleation sites are exhausted at an early stage of the crystallization. At the beginning of the transformation,

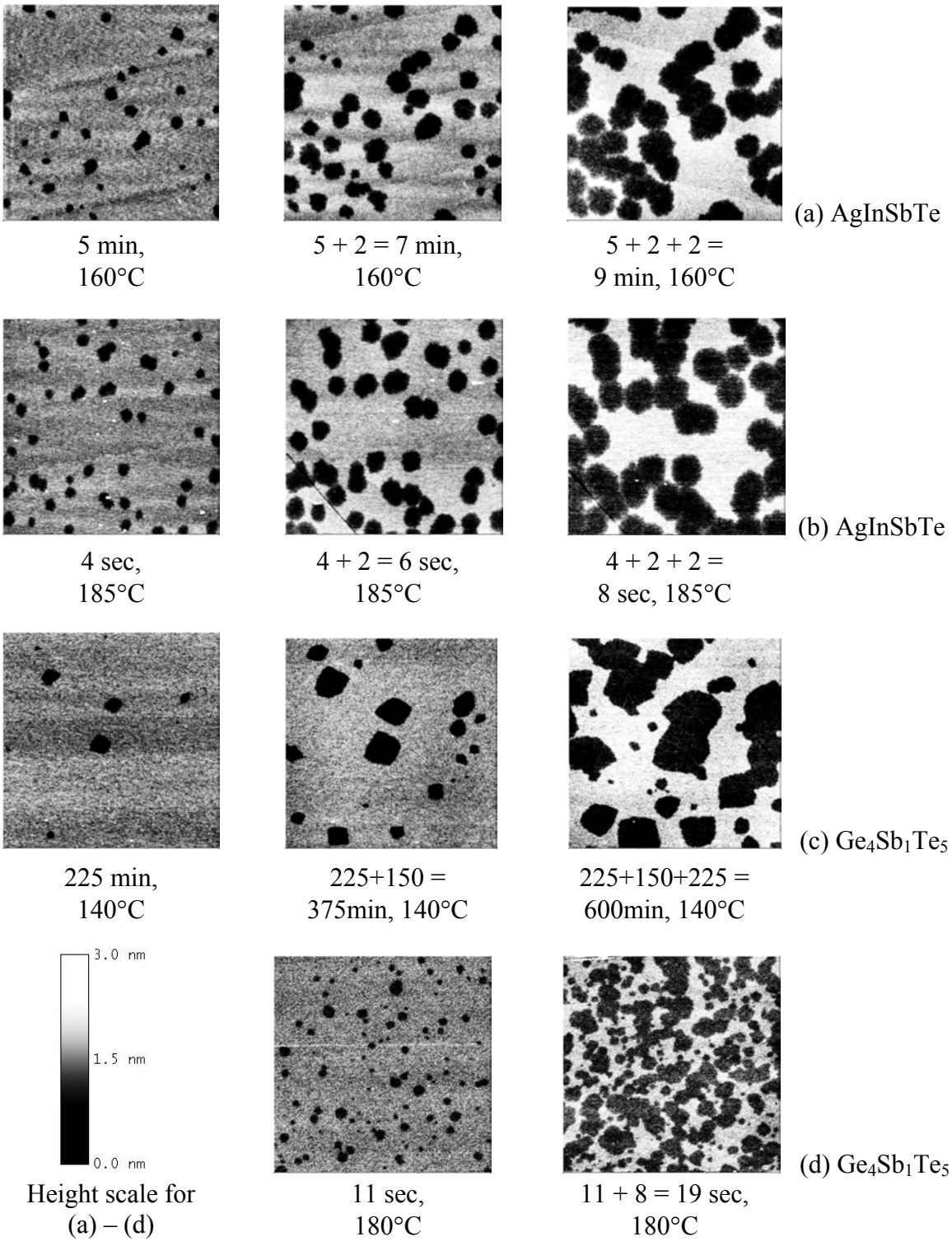

Figure 1. Atomic force microscope (AFM) scans: crystals (dark) are visible in amorphous surrounding (bright). Image dimensions: 3 μm by 3 μm. The height scale is given at the bottom on the left.

the nucleation rate increases from zero to a maximum value, and decreases to zero before about 30% of the sample surface is crystallized. Cross-sectional transmission electron microscopy [12] and optical reflectivity [13] show that crystals nucleate only heterogeneously at the (naturally oxidized) film surface. Similar sequences of AFM scans were performed after anneals at other temperatures (not shown). The total number of crystals per unit area was independent of temperature between 140°C and 185°C and found to be $N = (5.0 \pm 0.3)\ \mu m^{-2}$.

The crystal growth velocity could be determined from figure 1 (a) and 1 (b) for two stages of the transformation. Over the entire temperature range between 140°C and 185°C, the crystal growth velocity was independent of time. Therefore, we conclude that there is no composition change upon crystallization; growth is controlled by processes in the immediate vicinity of the interface (interface-controlled growth) [14]. If there were a change in composition upon crystallization (diffusion-controlled growth), the amorphous matrix around the crystal would be depleted in certain atoms, and the effective distances over which diffusion takes place may increase with increasing crystal size. In this case the growth velocity would decrease with time as $t^{(-1/2)}$ [14], which is not observed. Figure 2 is an Arrhenius plot of the crystal growth velocity, u. Apparently, crystal growth is thermally activated. DSC and immersion anneal data were fitted separately, so that the activation energy is not affected by a possible small difference in the temperature calibration between DSC furnace and oil bath. The weighted average of the two values for the activation energy, $E_u = (2.90 \pm 0.05)$ eV, is similar to the value of the total activation energy $E_{total} = (3.03 \pm 0.17)$ eV, which was obtained in the same temperature range from a Kissinger plot of the temperature dependence of the film resistance [10], and which should include components of both crystal nucleation and growth. Therefore, we conclude that the contribution of nucleation to the value of E_{total} is rather small. The value of E_u is more than a factor of two higher than the value for the isoconfigurational viscosity, $E_{visc} = (1.33 \pm 0.09)$ eV, which was measured between 60°C and 105°C [15]. Since the transport coefficients for viscous flow, diffusion and crystal growth are proportional, their activation energies should be the same. However, as the glass transition temperature T_g is usually accompanied by an *abrupt* change in activation energy [7-9], the data presented in figure 2 appear to be taken *above* T_g in the undercooled liquid: T_g depends on the timescale of the experiment [7-9] and may be significantly lower in these isothermal experiments than the value of T_g ~170°C -180°C determined in the earlier scanning experiments [16]. In contrast, the measurements presented in Ref. [15] were performed far below T_g in the amorphous phase. That the crystal growth velocity is time-independent between 140°C and 185°C points in the same direction: only in the amorphous phase, but not in the undercooled liquid, would a time dependence of the atomic transport rates be expected due to structural relaxation [8-9, 15].

B. $Ge_4Sb_1Te_5$

Figures 1 (c) and 1 (d) show AFM scans at 140°C and 180°C, respectively. As for AgInSbTe, nucleation for $Ge_4Sb_1Te_5$ was also observed to occur only heterogeneously at the (naturally oxidized) film surface [12-13], and the isothermal crystal growth velocity was observed to be time-independent (interface-controlled growth) and thermally activated between 140°C and 185°C. Figure 2 shows that the crystal growth velocity is of similar magnitude for both alloys. The weighted average of the activation energies obtained from DSC and immersion data, $E_u = (2.74 \pm 0.03)$ eV, is significantly lower than the value of the total activation energy $E_{total} = (3.48 \pm 0.12)$ eV, which was obtained in the same temperature range from a Kissinger

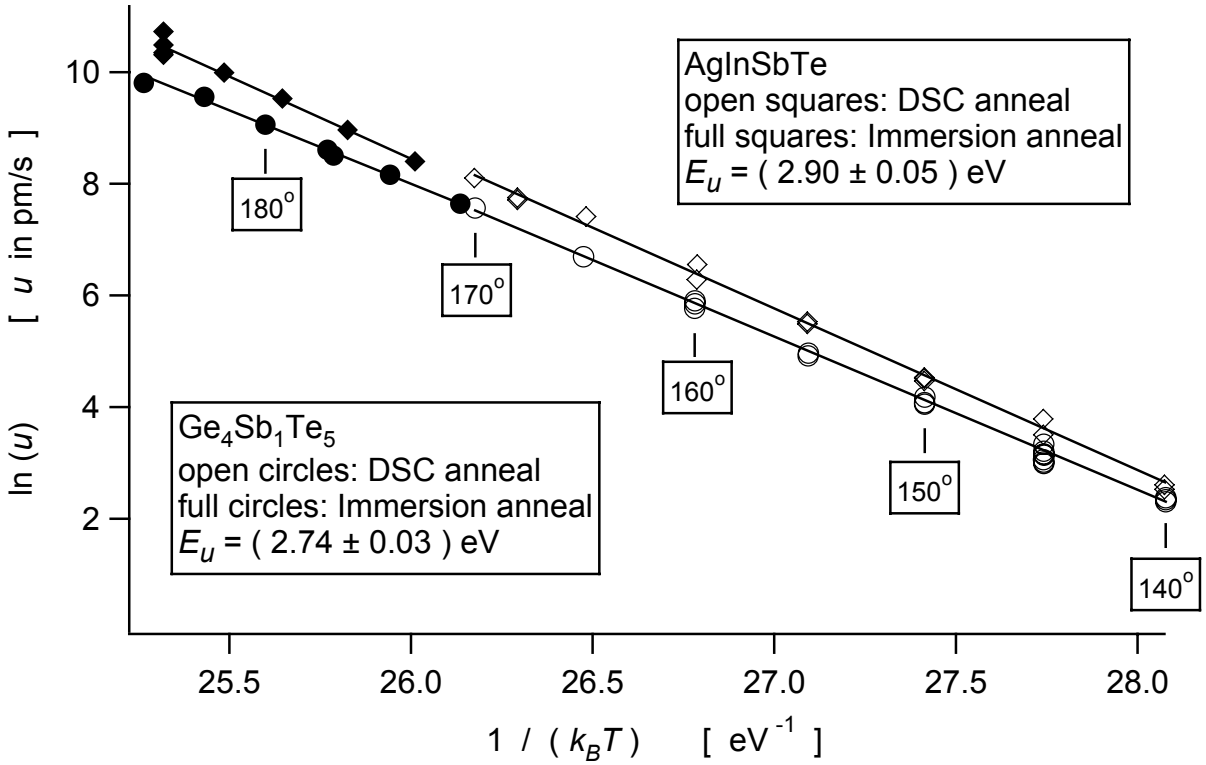

Figure 2. Crystal growth velocity u as a function of temperature T. The activation energies E_u were determined from the slopes of the Arrhenius fits. The lengths of the vertical error bars are on the order of the square/circle diagonals and are not indicated for clarity.

plot of the temperature dependence of the film resistance [11]. Therefore, we conclude that E_{total} includes a significant nucleation component. E_u is about 40% higher than the value for the isoconfigurational viscosity, E_{visc} = (1.94 ± 0.09) eV, which was measured between 60°C and 120°C [15]. This lets us draw the same conclusion as for AgInSbTe: the data of the crystal growth velocity for $Ge_4Sb_1Te_5$ were also taken in the undercooled liquid.

If figures 1 (c) and 1 (d) are compared with figures 1 (a) and 1 (b), two major differences between the two alloys are apparent. First, the crystal diameter distribution is broad for $Ge_4Sb_1Te_5$ only. Therefore, heterogeneous nucleation sites are not exhausted until the end of the transformation only for $Ge_4Sb_1Te_5$, i.e. the nucleation rate remains non-zero at all times. Second, the total number of crystals that would be observed after complete crystallization of the sample surface (per unit area) increases with increasing temperature for $Ge_4Sb_1Te_5$ only. These two differences qualitatively explain the observations of re-crystallization mechanisms mentioned in the introduction of this article [1, 3]: The small and temperature-independent number of crystals for AgInSbTe makes amorphous laser-induced marks of this alloy re-crystallize by the growth of the crystalline phase from the rim of the amorphous bit (growth-dominated re-crystallization). In contrast, that the number of crystals increases with increasing temperature for $Ge_4Sb_1Te_5$ implies nucleation-dominated re-crystallization particularly in the (extrapolated) regime of even higher temperatures, where laser-induced re-crystallization of amorphous marks takes place. Therefore, $Ge_4Sb_1Te_5$ re-crystallizes by nucleation and subsequent growth of crystals inside the amorphous bit.

CONCLUSIONS

The two phase change materials AgInSbTe and $Ge_4Sb_1Te_5$ exhibit *similar* crystal growth characteristics but *different* nucleation characteristics. Therefore, the difference in their crystal nucleation rate rather than the difference in their crystal growth velocity qualitatively explains the different re-crystallization mechanisms observed upon laser-induced annealing [1, 3].

The crystallization parameters determined in this project may be useful for simulating re-crystallization processes, as the data were collected in the temperature regime of the undercooled liquid (above T_g), where re-crystallization of laser-induced amorphous marks also takes place. However, care *still* has to be taken when extrapolating the data presented in figure 2 to higher temperatures: In the undercooled liquid, a Fulcher-Vogel type temperature dependence of the growth velocity applies sufficiently below the melting temperature, in which the (apparent) activation energy continuously decreases with increasing temperature [8-9]. Therefore, only upper limits of the growth velocities can be obtained from extrapolation with our activation energies to higher temperatures; the deviation increases with increasing temperature.

ACKNOWLEDGMENTS

We thank H. Dieker for help with the sample preparation. One of the authors (J. K.) acknowledges the Deutscher Akademischer Austauschdienst and the Studienstiftung des Deutschen Volkes for financial support. One of the authors (F. S.) acknowledges partial support from the Alexander-von-Humboldt-Stiftung. One of the authors (M. W.) acknowledges financial support from the Fonds der Chemischen Industrie.

REFERENCES

1. H. J. Borg, M. van Schijndel, J. C. N. Rijpers et al., Jpn. J. Appl. Phys. **40**, 1592 (2001).
2. N. Yamada, E. Ohno, K. Nishiuchi, et al., J. Appl. Phys. **69**, 2849 (1991).
3. J. H. Coombs, A. P. J. M. Jongenelis, W. van Es-Spiekman, and B. A. J. Jacobs, J. Appl. Phys. **78**, 4918 (1995).
4. C. Peng, L. Cheng, and M. Mansuripur, J. Appl. Phys. **82**, 4183 (1997).
5. A. C. Sheila and T. E. Schlesinger, J. Appl. Phys. **91**, 2803 (2002).
6. E. R. Meinders, H. J. Borg, M. H. R. Lankhorst, J. Hellmig, and A. V. Mijiritskii, J. Appl. Phys. **91**, 9794 (2002).
7. W. Kauzmann, Chem. Rev. **43**, 219 (1948).
8. F. Spaepen, in *Physics of Defects*, edited by R. Balian, M. Kleman, and J.-P. Poirier (Les Houches Lectures XXXV, North-Holland, Amsterdam, 1981), pp. 136-174.
9. F. Spaepen and D. Turnbull, Ann. Rev. Phys. Chem. **35**, 241 (1984).
10. W. K. Njoroge and M. Wuttig, J. Appl. Phys. **90**, 3816 (2001).
11. D. Wamwangi, W. K. Njoroge, and M. Wuttig, Thin Solid Films **408**, 310 (2002).
12. J. Kalb, C.-Y. Wen, F. Spaepen, and M. Wuttig, unpublished.
13. T.P. Leervad Pedersen, PhD thesis, RWTH Aachen, Germany (2003).
14. J. W. Christian, in *The Theory of Transformations in Metals and Alloys* (Pergamon Press, North-Holland, Amsterdam, 2nd edition, 1975), Chapter 11.
15. J. Kalb, F. Spaepen, T.P. Leervad Pedersen, and M. Wuttig, J. Appl. Phys. **94**, 4908 (2003).
16. J. Kalb, F. Spaepen, and M. Wuttig, J. Appl. Phys. **93**, 2389 (2003).